

NASA Technical Memorandum 83604

# Frictional and Morphological Properties of Au-MoS<sub>2</sub> Films Sputtered from a Compact Target

Talivaldis Spalvins  
*Lewis Research Center  
Cleveland, Ohio*

Prepared for the  
Eleventh International Conference on Metallurgical Coatings  
sponsored by the American Vacuum Society  
San Diego, California, April 9-13, 1984



FRICTIONAL AND MORPHOLOGICAL PROPERTIES OF Au-MoS<sub>2</sub> FILMS

SPUTTERED FROM A COMPACT TARGET

Talivaldis Spalvins

National Aeronautics and Space Administration

Lewis Research Center

Cleveland, Ohio 44135

SUMMARY

Au-MoS<sub>2</sub> films 0.02 to 1.2  $\mu\text{m}$  thick were sputtered from target compacted from 5 wt.% Au + 95 wt.% MoS<sub>2</sub>, to investigate the frictional and morphological film growth characteristics. The gold dispersion effects in MoS<sub>2</sub> films are of interest to increase the densification and strengthening of the film structure. Three microstructural growth stages were identified on the nano-micro-macrostructural level. During sliding both sputtered Au-MoS<sub>2</sub> and MoS<sub>2</sub> films have a tendency to break within the columnar region. The remaining or effective film, about 0.2  $\mu\text{m}$  thick, performs the lubrication. The Au-MoS<sub>2</sub> films displayed a lower friction coefficient with a high degree of frictional stability and less wear debris generation as compared to pure MoS<sub>2</sub> films. The more favorable frictional characteristics of the Au-MoS<sub>2</sub> films are attributed to the effective film thickness and the high density packed columnar zone which has a reduced effect on the fragmentation of the tapered crystallites during fracture.

INTRODUCTION

The tribological properties of the sputtered MoS<sub>2</sub> films are strongly influenced by their crystalline-amorphous nature, morphological growth, and compositional structure<sup>1-4</sup>. To achieve effective lubrication with sputtered MoS<sub>2</sub> films, two requirements have to be met: (1) a strong film/substrate adherence, and (2) a low crystalline slip during shearing.

All solid film lubrication theories are based on the conditions that there is no slip between the lubricant and the substrate solid surface. This implies that the adhesive forces between the substrate and the neighboring  $\text{MoS}_2$  molecule are sufficiently strong to prevent their detachment by the shear stresses developed in the films. A low shear strength in the  $\text{MoS}_2$  crystal thus ensures a relatively low friction.

Sputtered  $\text{MoS}_2$  films have been characterized to their morphological growth patterns on the nano-micro-macrostructural level. During the nucleation and growth process, the sputtered  $\text{MoS}_2$  films develop three distinct growth zones in respect to their film thicknesses<sup>5</sup>. When the sputtered  $\text{MoS}_2$  films (about 1  $\mu\text{m}$  thick) come in sliding contact with another surface they have a tendency to break within the columnar zone on the first sliding pass. Consequently, the lubrication is primarily performed by the remaining film which is about 0.2  $\mu\text{m}$  thick and is the effective lubricating film. This implies that the adhesive forces between the substrate and the  $\text{MoS}_2$  film are stronger than the cohesive forces in the columnar structure.

To strengthen the structural integrity of the  $\text{MoS}_2$  film in the columnar zone and possibly increase the thickness of the remaining or effective film, gold dispersion was introduced into the  $\text{MoS}_2$  film for film densification and strengthening purposes. A compact Au- $\text{MoS}_2$  sputtering target was used to achieve the gold distribution within the  $\text{MoS}_2$  film. Only one similar study on metal dispersion within sputtered  $\text{MoS}_2$  films has been reported by Stupp<sup>6</sup>. In this study co-deposition was accomplished by simultaneously sputtering two separate targets (nickel and  $\text{MoS}_2$ ). In this dual target sputtering system the nickel composition was controlled by varying the power input to the metal target. The metallic composition range was 5 to 8 wt.%.

The objective of this study was to determine the frictional characteristics in vacuum at ambient temperatures and the morphological growth patterns

of Au-MoS<sub>2</sub> films sputtered from a single target in respect to pure sputtered MoS<sub>2</sub> films. The gold composition in the compact target was 5 wt.%.

## EXPERIMENTAL CONDITIONS

### Sputtering Conditions

The sputtering apparatus used in this investigation was an rf-diode system with a superimposed dc bias previously described in Ref. 7. The planar compact Au-MoS<sub>2</sub> sputtering target 12.7 cm in diameter and 0.6 cm thick was made by powder metallurgy techniques. The formulation of the compact Au-MoS<sub>2</sub> target was 5 and 95 percent by weight of Au and MoS<sub>2</sub> powder, respectively. Before sputter deposition the target was always cleaned and outgassed by presputtering until the pressure stabilized. The sputtering argon pressure was 20 millitorr, with a power density of 3.5 w/cm<sup>2</sup> and the average deposition rates were about 0.025  $\mu\text{m}/\text{min}$  for a target-to-substrate distance of 2.5 cm. The substrate temperatures were between 50° and 125° C and depended directly on the duration of sputtering. The substrates coated were highly polished nickel foils, microscopic glass slides, and AISI 440C stainless-steel disks which were subsequently used for friction testing. The 440C disk specimens were abraded on silicon carbide paper down to 600 grit. Then they were polished on a lapping wheel with 3  $\mu\text{m}$  alumina and finally polished with 1  $\mu\text{m}$  diamond paste. The resultant surface finish was 0.05 CLA (center line average) micrometers. During sputtering the temperature was monitored by a Chromel-Alumel thermocouple embedded in the disk, with the foils and microscopic glass slides mounted on the disk surface. The substrate surfaces were sputter cleaned before sputter deposition. The growth morphology and film structure in the 0.02 to 1.2  $\mu\text{m}$  range were examined by transmission electron microscopy (TEM), electron diffraction (ED), and scanning electron microscopy (SEM). The elemental composition was analyzed by energy dispersive X-ray spectroscopy (EDXS).

### Friction Testing

Frictional testing of the rf sputtered Au-MoS<sub>2</sub> and pure MoS<sub>2</sub> films was performed on a pin-on-disk tribotester. The friction specimens consisted of a flat AISI 440C disk (6.25 cm diam) in sliding contact with a stationary, hemispherically tipped AISI 440C rider (0.476 cm radius). This configuration is widely used for solid film lubrication, since it provides extremely high contact stresses in contrast to the conforming type of contact. The Hertzian stress for the uncoated disk and pin contact at 2.45 newtons load was 122.5 kg/mm<sup>2</sup>. The sliding speed was 0.26 m/sec at a normal load of 2.45 newtons in a vacuum of 2x10<sup>-3</sup> torr.

### CRYSTAL STRUCTURE OF MoS<sub>2</sub>

MoS<sub>2</sub> has a layer structure, where a plane of Mo atoms are arranged in an hexagonal array situated between two hexagonal layers of S atoms as shown in Fig. 1. Each atom of Mo is surrounded at equal distances by six S atoms placed at the corners of a triangular prism. The distance between the adjacent S layers is larger (3.49 Å) than the actual thickness of a lamella (3.17 Å). As a result the inter-lamellar attractions between the adjacent lamellae are low and consist basically of weak Van der Walls interactions. However, the attraction between the Mo and S layers has a covalent nature. Consequently, the structural anisotropy of MoS<sub>2</sub> crystals results from the layered structure with strong bonding within the layers but considerably weaker Van der Walls interactions holding the layers together. The result is, that the MoS<sub>2</sub> crystals are easily cleaved to expose clean, ordered and almost molecularly smooth surfaces.

The basal or Van der Walls (0001) surfaces of MoS<sub>2</sub> have been studied with LEED and AES and the experimental results indicate that the Van der Walls surfaces were extremely resistant to reactions with oxygen and water vapor <sup>8-9</sup>.

However, the edge surfaces which are parallel to the C-axis are the active sites for adsorption. At these sites the Mo ions can exist in a number of different oxidation states<sup>10</sup>. The basic feature which controls and determines the exact  $\text{MoS}_2$  crystal structure is the chemical bonding which in turn is governed by complex electron interactions between the neighboring atoms. The strong polarization of S-atoms seems to be the main reason that  $\text{MoS}_2$  crystallizes in a layer lattice.

## RESULTS AND DISCUSSION

### Growth Micromorphology

Three micromorphological growth patterns of the sputtered  $\text{Au-MoS}_2$  films in the thickness range of 0.02 to 2  $\mu\text{m}$  were identified by TEM, ED, and SEM in terms of film thickness: (1) ridge or needle formation stage during nucleation, (2) equiaxed transition zone, and (3) densely packed columnar structure. These three growth zones identified for the  $\text{Au-MoS}_2$  films were previously also identified for pure  $\text{MoS}_2$  films and are schematically illustrated in Fig. 2. When each of the growth zones of  $\text{Au-MoS}_2$  and  $\text{MoS}_2$  films are carefully compared, several distinct microstructural differences do exist, but the most pronounced differences in the film behavior are to applied loads and stresses which are illustrated and discussed below.

The micromorphology of the ultra thin sputtered  $\text{Au-MoS}_2$  films (0.02 to 0.05  $\mu\text{m}$ ) during the nucleation state form the characteristic ridge formation morphology. Typical TEM micrographs of sputtered compact  $\text{Au-MoS}_2$  and pure  $\text{MoS}_2$  films (0.04  $\mu\text{m}$  thick) are shown in Fig. 3. The formation of the black ridges or needles is explained in terms of microcrystallite preferred orientation and curling or rolling-up effects as observed by stereomicroscopy. The microplatelets with the basal planes perpendicular to the substrate create the dark ridges or needles. Microplatelets with basal planes parallel to the substrate display the grey areas. A pronounced increase in the width of the

ridges by a factor of 2 to 3 is observed with the compact  $\text{Au-MoS}_2$  films as compared to the pure  $\text{MoS}_2$  films. When this ridge or needle type structure comes in stationary contact or is rubbed with another surface a complete morphological change occurs. The morphological structure after contact is shown by a TEM in Fig. 4 for  $\text{Au-MoS}_2$  film. The characteristic ridge type structure changed into an agglomeration of widely assorted spheroidal-like particles within the range of 30 to 60  $\text{\AA}$  in size. Electron diffraction patterns also confirmed a change in crystallographic orientation after rubbing.

As the film thickness increases to over 0.07  $\mu\text{m}$ , the ridge type structure grows into an equiaxed transition zone with strong cohesive forces, before it grows finally into a densely packed columnar structural network. A typical SEM cross section of the compact  $\text{Au-MoS}_2$  film and the pure  $\text{MoS}_2$  film is shown in Fig. 5. The compact  $\text{Au-MoS}_2$  film structure has the fibers or platelets more densely packed as compared to the pure  $\text{MoS}_2$  film. The pure  $\text{MoS}_2$  columnar structure consists of tapered longitudinal platelets about 0.25  $\mu\text{m}$  in diameter which are separated by open voided longitudinal boundaries few 100  $\text{\AA}$  in width. This particular structure also has a high dislocation density and has a high level of residual stresses.

#### Correlation Between Friction and Micromorphology

Typical friction traces for sputtered 5 wt.%  $\text{Au-MoS}_2$  and sputtered  $\text{MoS}_2$  films are shown in Fig. 6. By comparing these two traces the compact  $\text{Au-MoS}_2$  films display several favorable frictional characteristics: (1) a slightly lower coefficient of friction and (2) a higher degree of frictional stability without generating any frictional irregularities in terms of a fluctuating coefficient of friction. It should be noted that the coefficient of friction for the compact  $\text{Au-MoS}_2$  film is very steady during the sliding, has a lower frictional amplitude and reaches a steady-state frictional condition.

When the two wear tracks of the respective films are compared after a few cycles of sliding a distinct difference in the film fracture and the generation of the wear debris is observed as shown in Fig. 7. The Au-MoS<sub>2</sub> film after fracture has a tendency to break or spall in large segments, without undergoing the fiber fragmentation, characteristic for the pure MoS<sub>2</sub> film. Because of the longitudinal porosity between the tapered crystallites a large volume of wear debris is generated for the MoS<sub>2</sub> film. It should be remembered that the remaining or the effective film after fracture determines the effectiveness of lubrication, and this film region is basically the equiaxed zone.

The morphological growth zones for the Au-MoS<sub>2</sub> and MoS<sub>2</sub> films are schematically illustrated after sliding in respect to film fracture and film fragmentation in the columnar zone in Fig. 8. The film fracture always occurs in the columnar zone for Au-MoS<sub>2</sub> and MoS<sub>2</sub> films since this structure is very sensitive to spalling or breaking off. However, a distinct difference exists in the cohesiveness between the Au-MoS<sub>2</sub> and MoS<sub>2</sub> films during fracture. The pure MoS<sub>2</sub> films after sliding due to their high degree of longitudinal porosity tend to disintegrate as tapered columns or fibers as shown in Fig. 8. After the separation of the columnar structure the remaining or effective film is about 0.2  $\mu\text{m}$  thick, and this region of the film performs the actual lubrication. The Au-MoS<sub>2</sub> film during fracture does not disintegrate into a large number of individual fibers, but only into a few large fragments. The high degree of cohesiveness which exists in between the tapered crystallites prevents disintegration. Preliminary results also indicate that the effective or remaining film is of the same thickness as the pure MoS<sub>2</sub> film, namely 0.2  $\mu\text{m}$ .

#### CONCLUSIONS

The structural growth morphology and the frictional characteristics of sputtered Au-MoS<sub>2</sub> films were determined and compared to sputtered MoS<sub>2</sub>

films. Three structural growth morphologies in the thickness range 0.02 to 1.2  $\mu\text{m}$  were identified by TEM and SEM: (1) a ridge formation zone, (2) an equiaxed transition zone, and (3) a densely packed columnar zone. The co-sputtered Au-MoS<sub>2</sub> films displayed a lower and more stable coefficient of friction than the pure MoS<sub>2</sub> films. During sliding the breakup of the films always occurs in the columnar zone for both Au-MoS<sub>2</sub> and MoS<sub>2</sub>. Due to the higher columnar packing density in the Au-MoS<sub>2</sub> films, the separated Au-MoS<sub>2</sub> film after fracture does not disintegrate into a large volume of individually tapered crystallites as does the MoS<sub>2</sub> sputtered film. As a result less wear debris is generated as compared to pure MoS<sub>2</sub> films.

#### REFERENCES

1. T. Spalvins, ASLE Trans., 17, 1 (1974).
2. M. T. Lavik and M. E. Campbell, ASLE Trans., 15, 233 (1972).
3. M. Nishimura, M. Nosaka, M. Suzuki, and Y. Miyakawa, Proceedings of the 2nd International Conference on Solid Lubrication, Denver (American Society of Lubrication Engineers, Park Ridge, IL., 1978), p. 128.
4. R. I. Christy and H. R. Ludwig. Thin Solid Films, 64, 223-229 (1979).
5. T. Spalvins, Thin Solid Films, 96, 17-24 (1982).
6. B. C. Stupp, Thin Solid Films, 84, 257-266 (1981).
7. T. Spalvins, ASLE Trans., 14, 267 (1971).
8. R. H. Williams and A. J. McEwvoy, J. Phys. D4 (1971).
9. H. C. Feng and J. M. Chen, J. Phys. C7 (1974) L75.
10. K. Suzuki et al., J. Electron Spectroscopy and Related Phenomena, 24, 283-287 (1981).

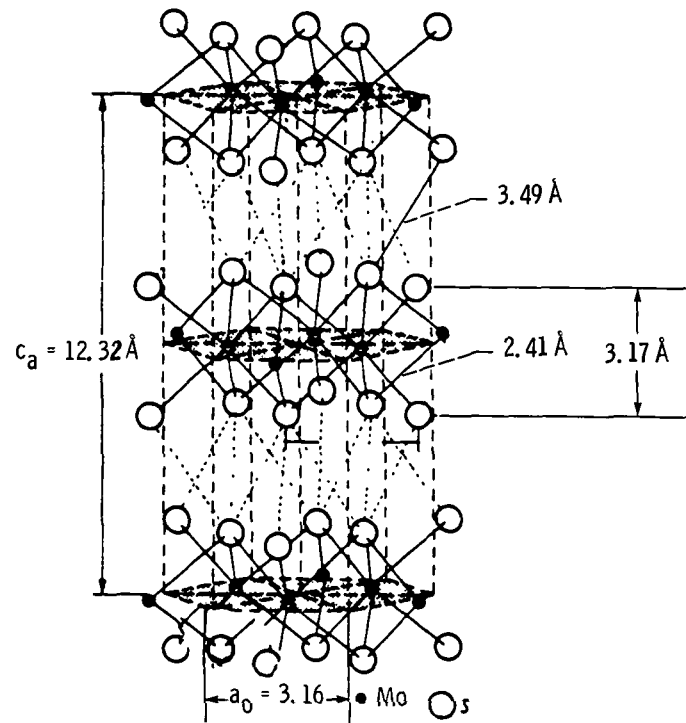


Figure 1. - Structure of  $\text{MoS}_2$ .

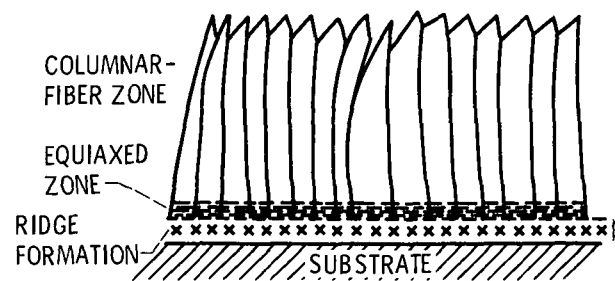
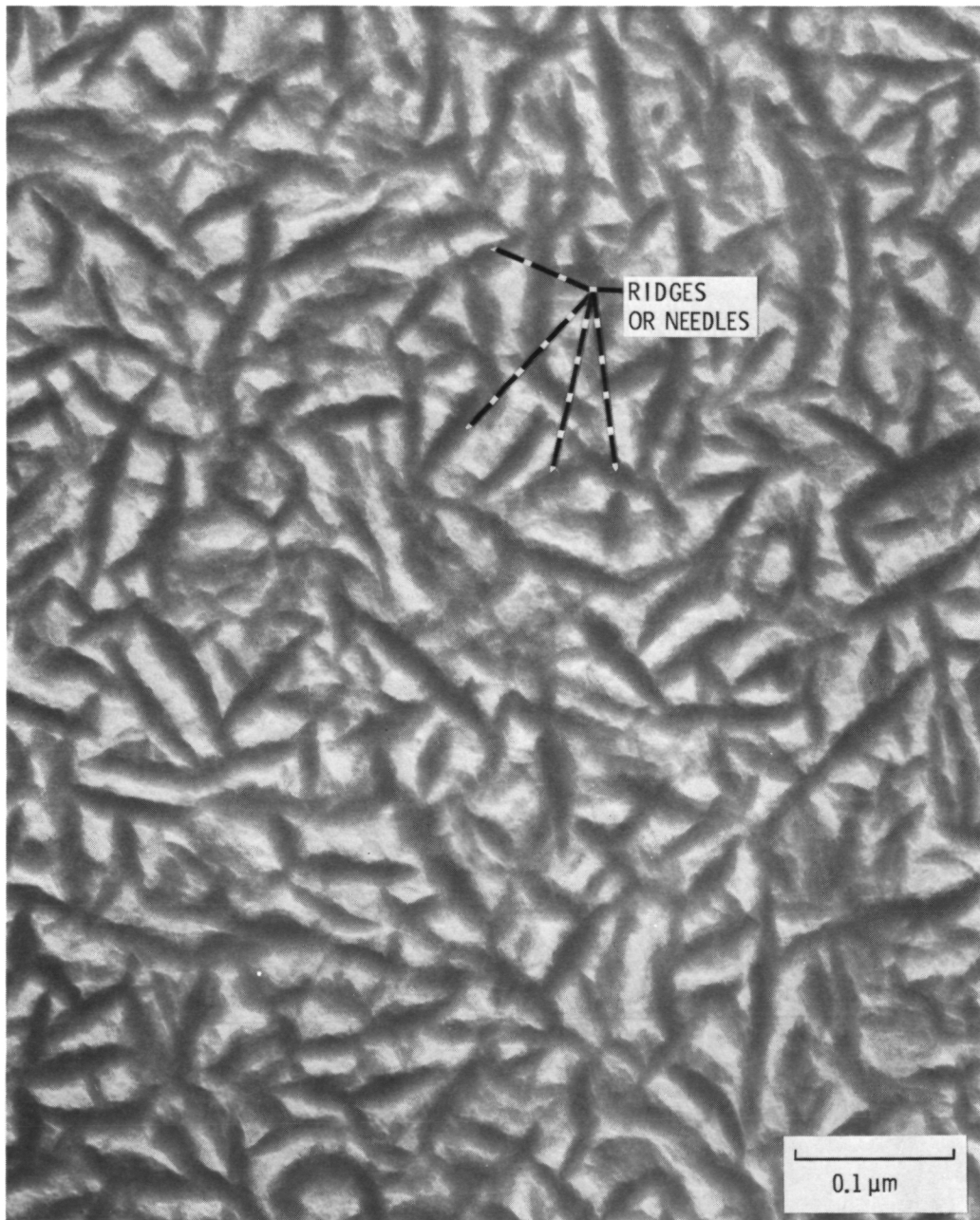


Figure 2. - Schematic sketch of the morphological growth zones of sputtered  $\text{Au-MoS}_2$  and  $\text{MoS}_2$  films.



(a) 5 wt. % Au-MoS<sub>2</sub>.

Figure 3. - TEM micrographs of sputtered Au-MoS<sub>2</sub> and pure MoS<sub>2</sub> films.



(b)  $\text{MoS}_2$ .

Figure 3. - Concluded.

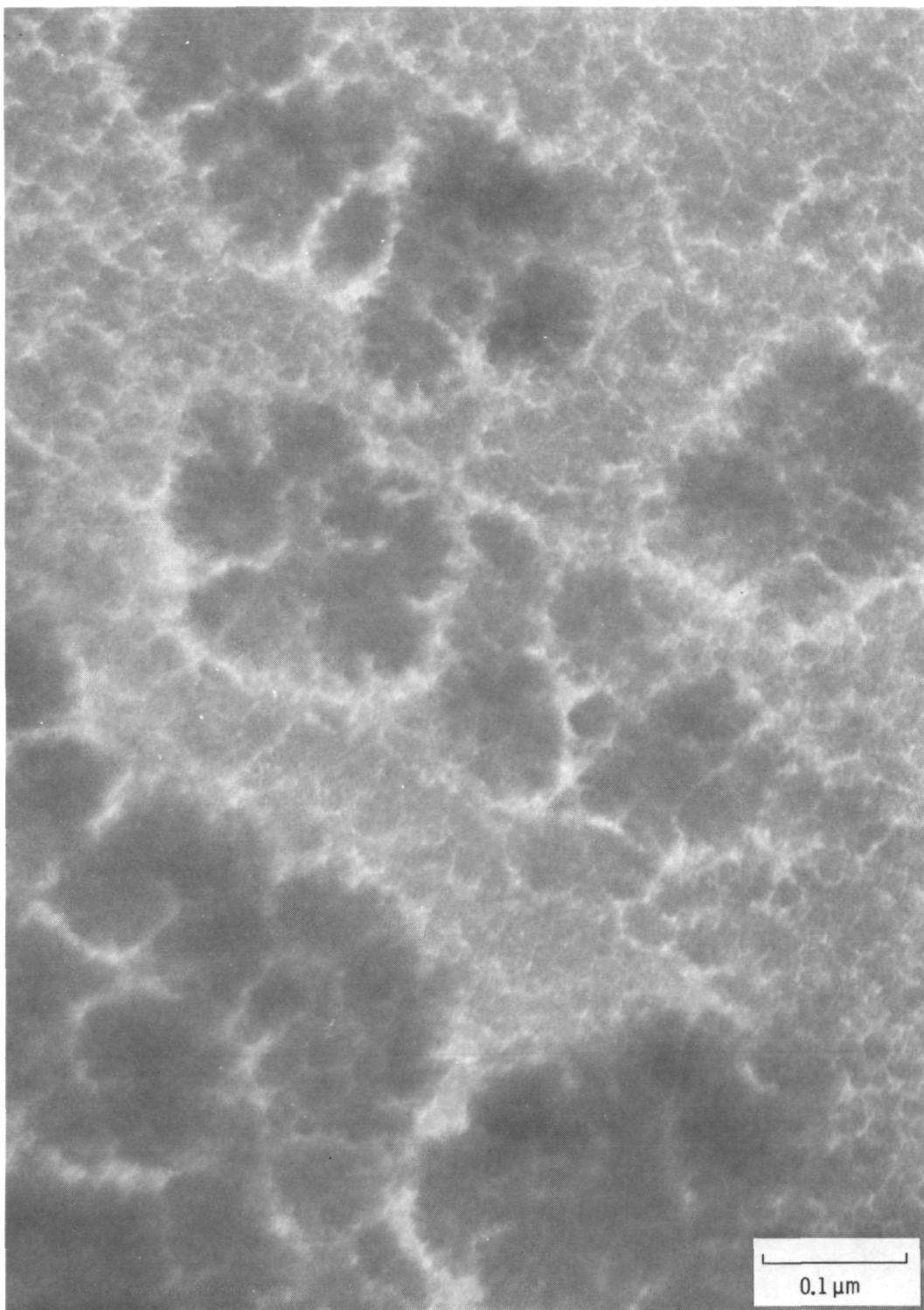
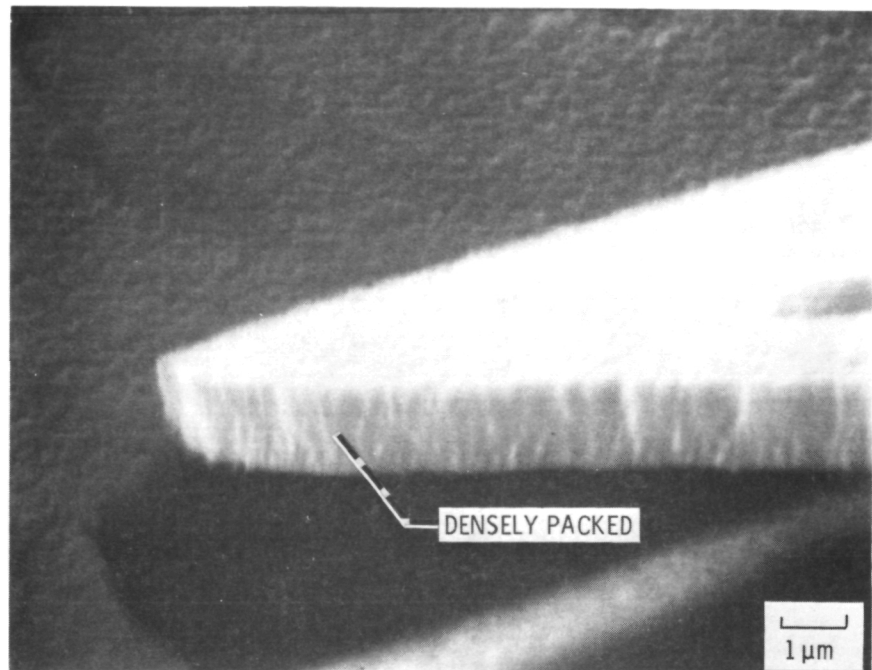
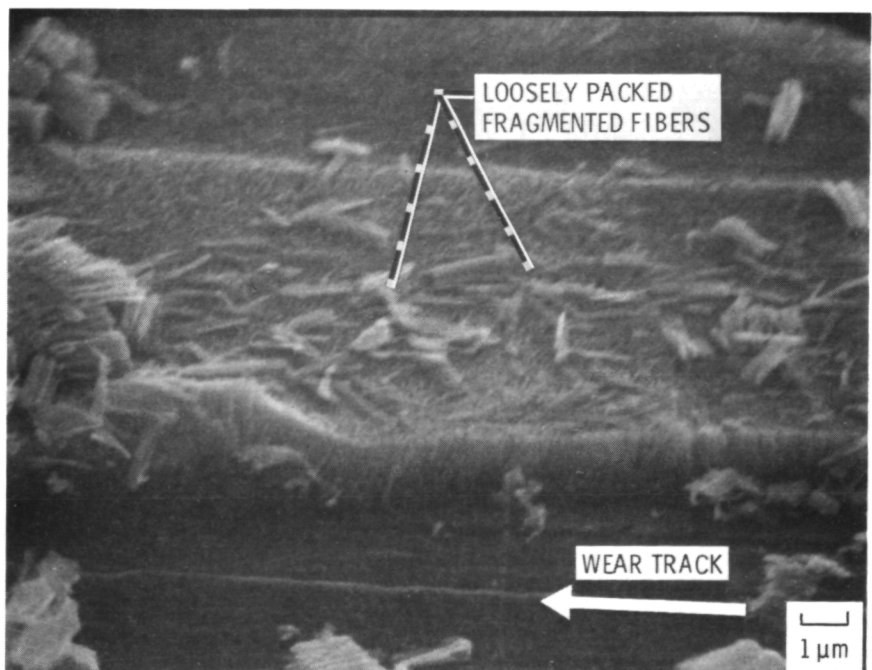


Figure 4. - TEM of co-sputtered Au-MoS<sub>2</sub> film after rubbing.

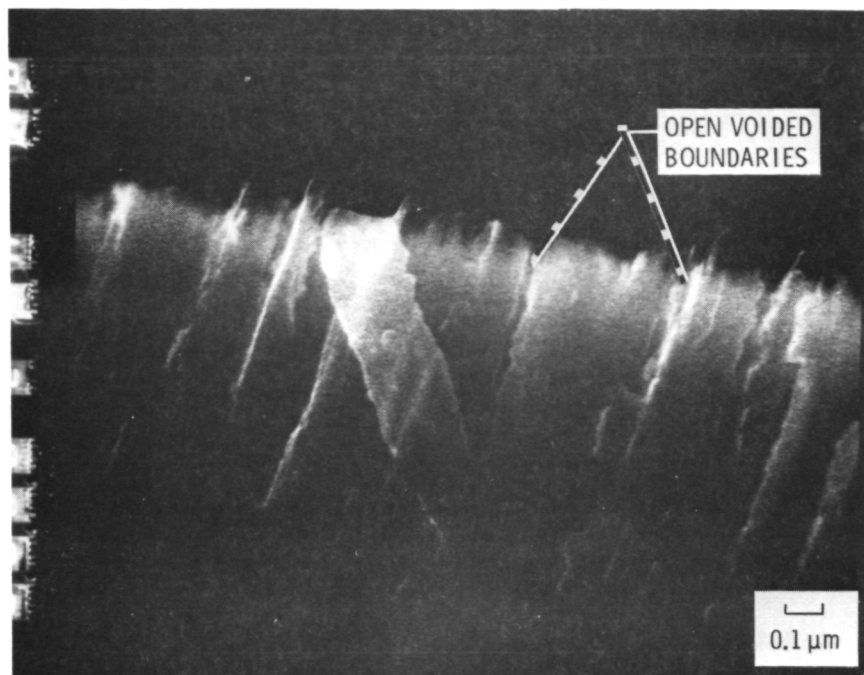


(a) Au-MoS<sub>2</sub> film.



(b) MoS<sub>2</sub> film.

Figure 5. - SEM cross-sectional structure of sputtered Au-MoS<sub>2</sub> and MoS<sub>2</sub> films.



(c)  $\text{MoS}_2$  film.

Figure 5. - Concluded.

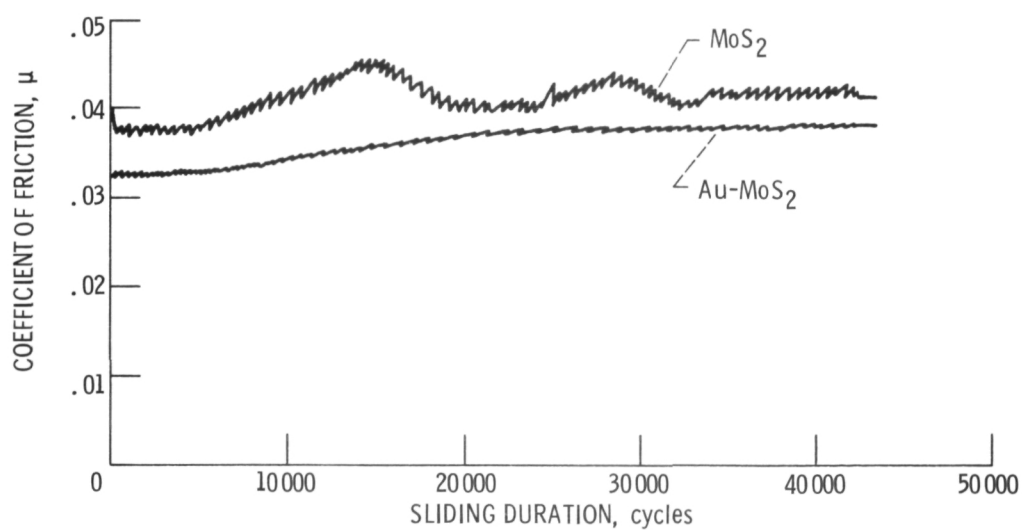
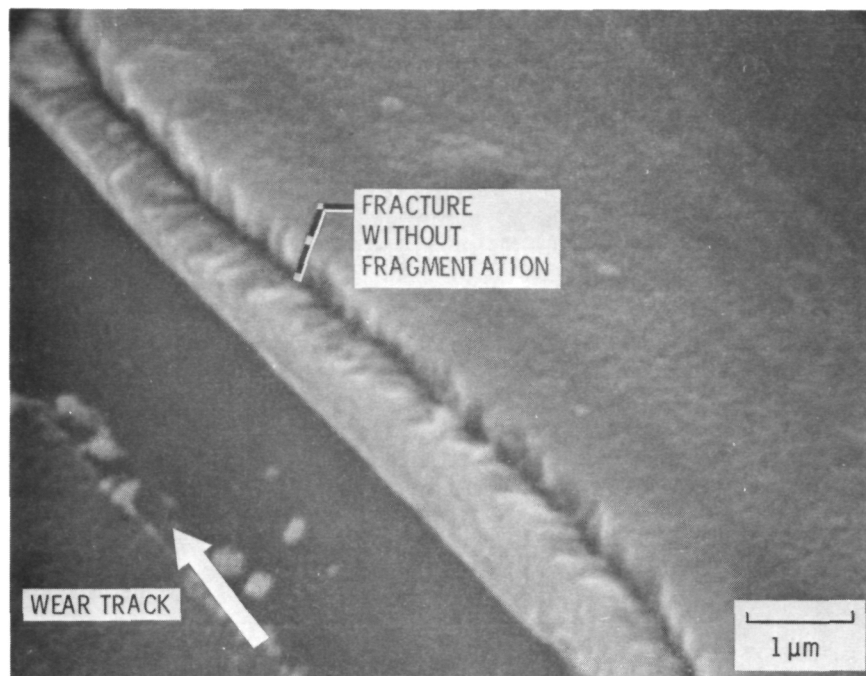
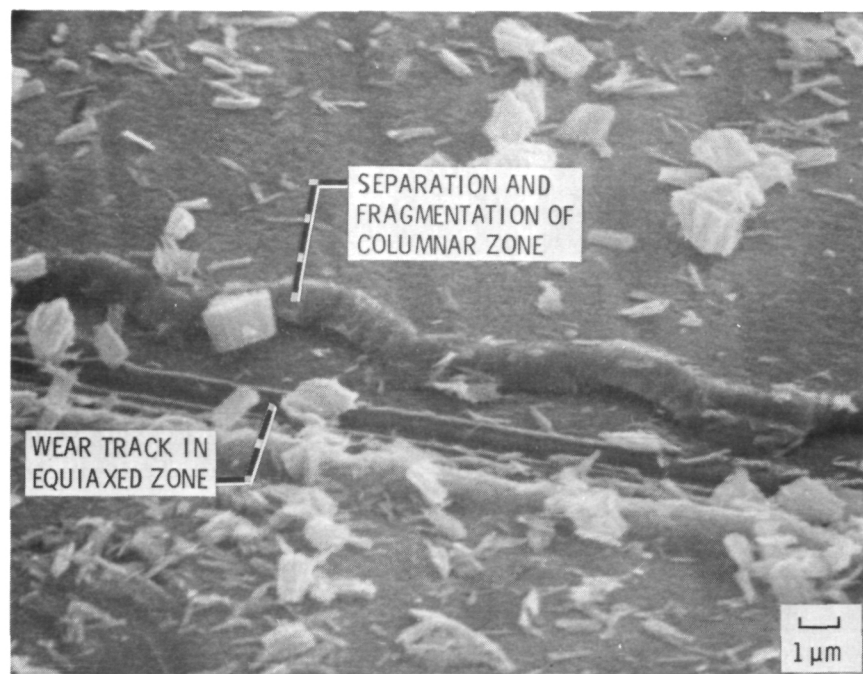


Figure 6. - Comparison of typical friction traces of  $\text{Au}-\text{MoS}_2$  and pure  $\text{MoS}_2$  films 0.2  $\mu\text{m}$  thick on 440 C surface.



(a) Au-MoS<sub>2</sub> film.



(b) MoS<sub>2</sub> films.

Figure 7. - Film fracture and wear debris after sliding.

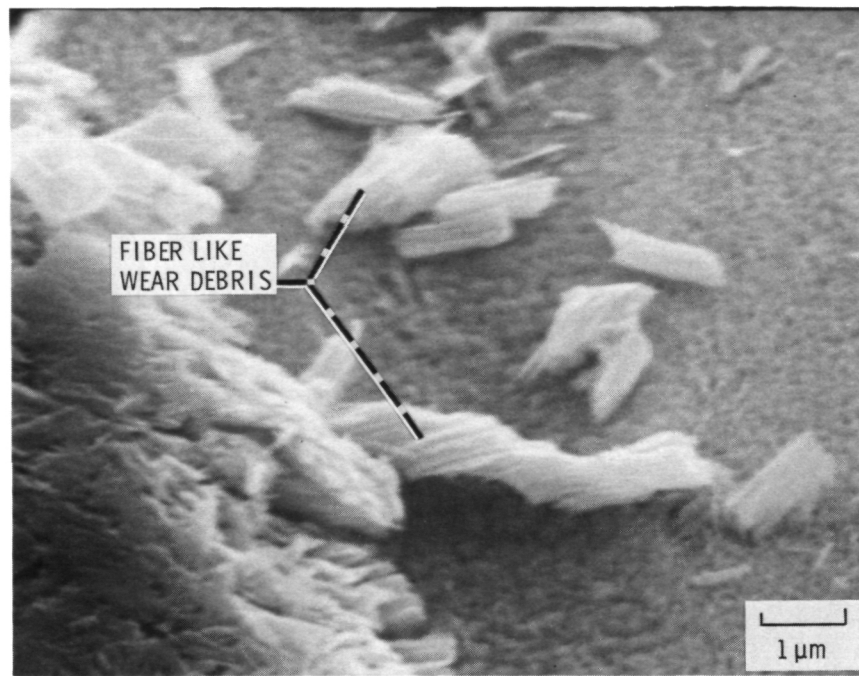


Figure 7. - Concluded.

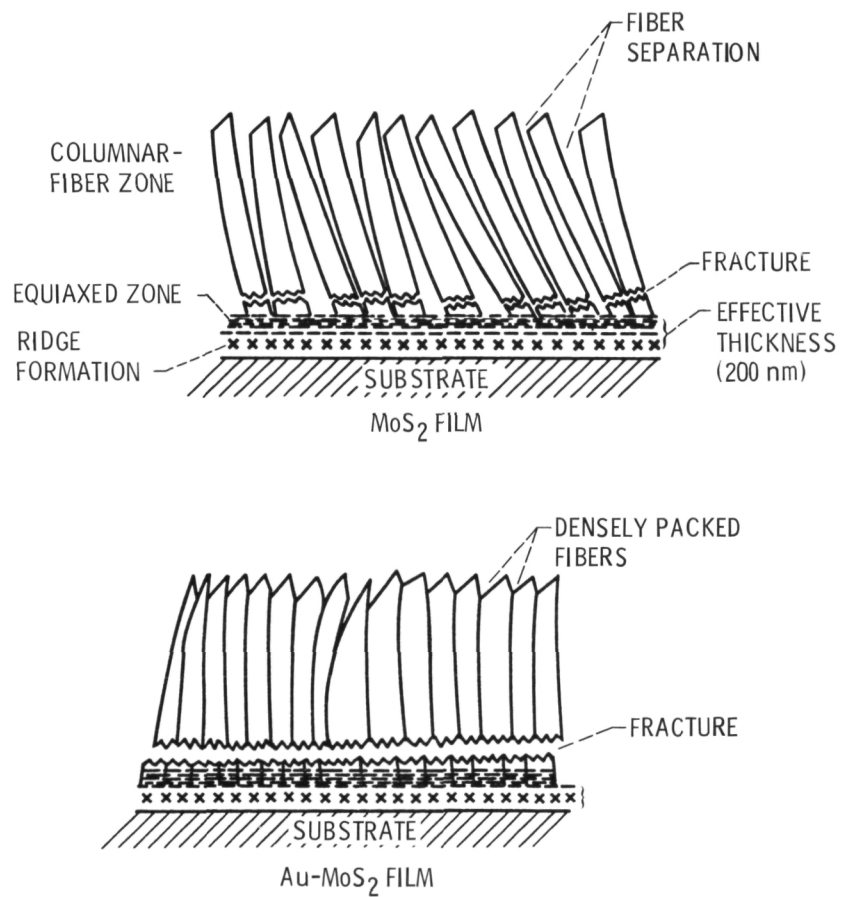


Figure 8. - Schematic sketches of fracture and film fragmentation in the columnar zone.

1. Report No. NASA TM-83604	2. Government Accession No.	3. Recipient's Catalog No.	
4. Title and Subtitle  Frictional and Morphological Properties of Au-MoS <sub>2</sub> Films Sputtered from a Compact Target		5. Report Date	
		6. Performing Organization Code 506-53-1B	
7. Author(s)  Talivaldis Spalvins		8. Performing Organization Report No. E-2004	
		10. Work Unit No.	
9. Performing Organization Name and Address  National Aeronautics and Space Administration Lewis Research Center Cleveland, Ohio 44135		11. Contract or Grant No.	
		13. Type of Report and Period Covered Technical Memorandum	
12. Sponsoring Agency Name and Address  National Aeronautics and Space Administration Washington, D.C. 20545		14. Sponsoring Agency Code	
15. Supplementary Notes  Prepared for the Eleventh International Conference on Metallurgical Coatings sponsored by the American Vacuum Society, San Diego, California, April 9-13, 1984.			
16. Abstract  Au-MoS <sub>2</sub> films 0.02 to 1.2 $\mu$ m thick were sputtered from target compacted from 5 wt.% Au + 95 wt.% MoS <sub>2</sub> , to investigate the frictional and morphological film growth characteristics. The gold dispersion effects in MoS <sub>2</sub> films are of interest to increase the densification and strengthening of the film structure. Three microstructural growth stages were identified on the nano-micro-macrostructural level. During sliding both sputtered Au-MoS <sub>2</sub> and MoS <sub>2</sub> films have a tendency to break within the columnar region. The remaining or effective film, about 0.2 $\mu$ m thick, performs the lubrication. The Au-MoS <sub>2</sub> films displayed a lower friction coefficient with a high degree of frictional stability and less wear debris generation as compared to pure MoS <sub>2</sub> films. The more favorable frictional characteristics of the Au-MoS <sub>2</sub> films are attributed to the effective film thickness and the high density packed columnar zone which has a reduced effect on the fragmentation of the tapered crystallites during fracture.			
17. Key Words (Suggested by Author(s))  Lubrication Sputtering Morphology		18. Distribution Statement  Unclassified - unlimited STAR Category 37	
19. Security Classif. (of this report) Unclassified	20. Security Classif. (of this page) Unclassified	21. No. of pages	22. Price*

National Aeronautics and  
Space Administration

Washington, D.C.  
20546

Official Business

Penalty for Private Use, \$300

SPECIAL FOURTH CLASS MAIL  
BOOK



Postage and Fees Paid  
National Aeronautics and  
Space Administration  
NASA-451

NASA

POSTMASTER: If Undeliverable (Section 154  
Postal Manual) Do Not Return

---